JOURNAL OF GUIDANCE, CONTROL, AND DYNAMICS
Vol. 19, No. 5, September–October 1996

Closed-Form Optimal Guidance Law for Missiles of Time-Varying Velocity

Hangju Cho* and Chang Kyung Ryoo†
Agency for Defense Development, Taejon 305-600, Republic of Korea
and
Min-Jea Tahk‡
Korea Advanced Institute of Science and Technology, Taejon 305-701, Republic of Korea

An optimal guidance law for missiles with time-varying velocity is investigated. The closed-form solution is derived and properties of the key variables of the solution, such as a time-to-go-like function and the time-varying guidance gain, are studied. Implementation aspects related to the computations of time-to-go and the guidance gain also are considered. Simulation studies show that the performance of the proposed guidance law is superior to that of proportional navigation or augmented proportional navigation.

Introduction

OPTIMAL homing guidance laws have been studied extensively for many years in an attempt to replace the well-known proportional navigation guidance (PNG) law that is still widely used in various forms for practical homing missile applications. Most optimal guidance laws (OGLs) have been derived from linear quadratic optimal control theory to obtain feedback-form solutions, and many of them take target maneuver into account to cope with highly maneuvering target scenarios.

On the other hand, we find only a few papers that explicitly consider missile velocity variations in deriving OGLs. Green et al.[1] studied the game-OGL for a coasting missile with a parabolic drag polar. Nazaroff[2] solved a linear quadratic optimization problem for a missile with longitudinal acceleration and jerk, but did not look into the characteristics of the resulting guidance law. When we turn our attention to a related problem—time-to-go estimation—we find some papers, such as those by Riggs[3] and Hull et al.,[4] that considered some particular types of missile longitudinal acceleration history during engagement. We also note a recent paper of Baba et al.,[5] where they studied a new guidance law, accounting for missile velocity changes during boost and coasting phases. Their result, however, is not based on an optimal guidance problem but on the philosophy of nullifying the line-of-sight (LOS) rate deviation from the one expected for the trajectory along the collision triangle.

We derive an OGL for a missile with an arbitrary velocity profile. It turns out that the resulting law can be put into the same form as the one for constant-velocity missiles. The difference is that our OGL has a time-varying guidance gain $N(t)$ and uses a t_{go} (time to go)-like function $t_g(t)$, in which the effect of the future missile velocity change is taken into account. Some efforts then are devoted to the study of the properties of these two guidance variables. Implementation aspects and some simulation results also are presented.

OGL

Consider the guidance geometry shown in Fig. 1. With respect to the reference line, σ_m and σ_t denote the flight-path angles of the missile and the target, respectively. Let σ_L be the initial launch angle or flight-path angle for the perfect collision path that remains fixed during missile guidance. The deviation of the missile flight-path angle from σ_L is defined by $\Delta\sigma_m = \sigma_m - \sigma_L$. The commanded missile acceleration is assumed to be normal to the missile velocity vector. The equations of motion for the homing problem then are given by

$$\dot{z}(t) = V_t(t)\sin\sigma_t(t) - V_m(t)\sin\sigma_m(t)$$
$$V_m(t)\dot{\sigma}_m(t) = u(t) \tag{1}$$

where z denotes the relative position from the reference line, V_m is the missile speed, and u is the magnitude of missile acceleration. We further assume that 1) V_t, $\dot{V}_t$ and σ_t, $\dot{\sigma}_t$ are known, 2) $\Delta\sigma_m$ is small, and 3) V_m and $\dot{V}_m = A_m$ are given.

Under these assumptions, we linearize Eqs. (1) about $z = 0$ and $\sigma_m = \sigma_L$ to obtain

$$\dot{z}(t) = V_t(t)\sin\sigma_t(t) - V_m(t)\sin\sigma_L - V_m(t)\cos\sigma_L\Delta\sigma_m(t)$$
$$V_m(t)\Delta\dot{\sigma}_m(t) = u(t) \tag{2}$$

Define

$$V_z \equiv V_t\sin\sigma_t - V_m\sin\sigma_L - V_m\cos\sigma_L\Delta\sigma_m$$

$$a \equiv \frac{\dot{V}_m}{V_m}, \qquad a_{tz} \equiv \frac{\mathrm{d}}{\mathrm{d}t}(V_t\sin\sigma_t)$$

Then Eqs. (2) are equivalent to

$$\dot{z}(t) = V_z(t)$$
$$\dot{V}_z(t) = a(t)V_z(t) - a(t)V_t(t)\sin\sigma_t(t) - u_z(t) + a_{tz}(t) \tag{3}$$

where $u_z = u\cos\sigma_L$. Now, the objective is to find $u_z(t)$, minimizing

$$J = \frac{1}{2}\int_0^{t_f}[u_z(t)]^2\,\mathrm{d}t \tag{4}$$

subject to the terminal constraint $z(t_f) = 0$.

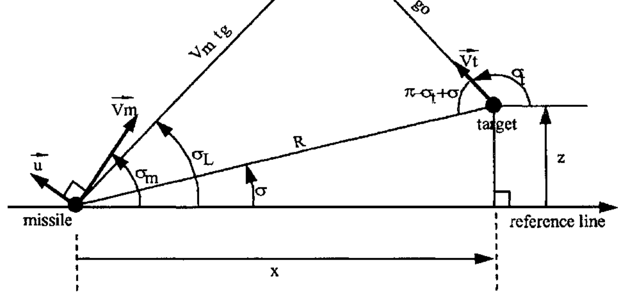

Fig. 1 Homing geometry.

Received June 7, 1995; revision received May 22, 1996; accepted for publication May 28, 1996.

*Senior Researcher, ADD 4-2-2, P.O. Box 35, Yusung.
†Researcher, ADD 4-2-2, P.O. Box 35, Yusung.
‡Associate Professor, Department of Aerospace Engineering, 373-1 Kusung Yusung. Member AIAA.

The solution of the optimal control problem posed in Eqs. (3) and (4) can be obtained in a straightforward manner[6] and is given as

$$u_z(t) = B^T F(t)[G(t)]^{-1}\left\{F^T(t)\begin{bmatrix} z(t) \\ V_z(t)\end{bmatrix} + \int_t^{t_f} F^T(s)\begin{bmatrix} 0 \\ -a(s)V_t(s)\sin\sigma_t(s) + a_{tz}(s)\end{bmatrix}\mathrm{d}s\right\} \tag{5}$$

where

$$\dot{F}(t) = -A^T(t)F(t), \qquad F(t_f) = \begin{bmatrix} 1 \\ 0 \end{bmatrix} \tag{6}$$

$$G(t) = -\int_t^{t_f} F^T(s)BB^T F(s)\,\mathrm{d}s \tag{7}$$

and

$$A(t) = \begin{bmatrix} 0 & 1 \\ 0 & a(t)\end{bmatrix}, \qquad B = \begin{bmatrix} 0 \\ -1 \end{bmatrix}$$

The preceding equations are solved to give

$$F(t) = \begin{bmatrix} 1 \\ t_g(t)\end{bmatrix}, \qquad G(t) = -\int_t^{t_f} t_g^2(s)\,\mathrm{d}s \tag{8}$$

where

$$t_g(t) = \frac{\int_t^{t_f} V_m(s)\,\mathrm{d}s}{V_m(t)} \tag{9}$$

and therefore

$$u_z(t) = -\frac{t_g(t)}{G(t)}\left[z(t) + t_g(t)V_z(t) - \int_t^{t_f} a(s)t_g(s)V_t(s)\sin\sigma_t(s)\,\mathrm{d}s + \int_t^{t_f} t_g(s)a_{tz}(s)\,\mathrm{d}s\right] \tag{10}$$

Equation (10) can be put into the form

$$u_z(t) = \frac{N(t)}{t_g^2(t)} \times \mathrm{ZEM}(t) \tag{11}$$

where ZEM denotes the zero effort miss and the guidance gain $N(t)$ is defined as

$$N(t) = -\frac{t_g^3(t)}{G(t)} = \frac{t_g^3(t)}{\int_t^{t_f} t_g^2(s)\,\mathrm{d}s} \tag{12}$$

The guidance law of Eq. (11) takes the same form as the OGL for constant missile velocity cases, but $t_g(t)$ instead of $t_{\mathrm{go}}(t)$ is used here to define $N(t)$. If we define $t_{\mathrm{go}} \equiv t_f - t$ and use $\dot{t}_g = -1 - at_g$, then

$$\int_t^{t_f} t_g(s)a_{tz}(s)\,\mathrm{d}s = [t_g(s)V_t(s)\sin\sigma_t(s)]_t^{t_f} - \int_t^{t_f}[-1 - a(s)t_g(s)]V_t(s)\sin\sigma_t(s)\,\mathrm{d}s$$

$$= -t_g(t)V_t(t)\sin\sigma_t(t) + \int_t^{t_f} V_t(s)\sin\sigma_t(s)\,\mathrm{d}s + \int_t^{t_f} a(s)t_g(s)V_t(s)\sin\sigma_t(s)\,\mathrm{d}s$$

so that ZEM can be expressed as

$$\mathrm{ZEM}(t) = z(t) + t_g(t)V_z(t) - t_g(t)V_t(t)\sin\sigma_t(t) + \int_t^{t_f} V_t(s)\sin\sigma_t(s)\,\mathrm{d}s = z(t) + t_g(t)V_z(t) - [t_g(t) - t_{\mathrm{go}}(t)]V_t(t)\sin\sigma_t(t) + \int_t^{t_f}\int_t^s a_{tz}(v)\,\mathrm{d}v\,\mathrm{d}s$$

Now, using $V_z \approx V_t\sin\sigma_t - V_m\sin\sigma_m$, we have

$$\mathrm{ZEM} = z + t_{\mathrm{go}}V_z + (t_{\mathrm{go}} - t_g)V_m\sin\sigma_m + \int_t^{t_f}\int_t^s a_{tz}(v)\,\mathrm{d}v\,\mathrm{d}s \tag{13}$$

Note that the OGL with the ZEM given by Eq. (13) is similar to that of augmented proportional navigation (APN) for intercepting an accelerating target. The only difference is the additional term $(t_{\mathrm{go}} - t_g)V_m\sin\sigma_m$ in Eq. (13), which accounts for the missile velocity variation. In fact, the longitudinal acceleration of the missile can be treated as a target acceleration in the opposite direction; thus, the equivalent target acceleration along the z axis is $-\dot{V}_m\sin\sigma_m$. Without control effort, $\sigma_m(t)$ remains constant. Hence, an additional term, which should be included in the ZEM of APN, is calculated as

$$-\int_t^{t_f}\int_t^s \dot{V}_m(v)\sin\sigma_m(v)\,\mathrm{d}v\,\mathrm{d}s = -\left[\int_t^{t_f}\int_t^s \dot{V}_m(v)\,\mathrm{d}v\,\mathrm{d}s\right]\sin\sigma_m(t) = (t_{\mathrm{go}} - t_g)V_m(t)\sin\sigma_m(t)$$

which is just the additional term in Eq. (13). Note, however, that the guidance gain $N(t)$ in Eq. (12) is different from that of APN; the effect of the missile axial acceleration also is taken into account in $N(t)$.

The optimal control u_z can be expressed in terms of the costate $\lambda(t)$ as $u_z(t) = -B^T\lambda(t)$. Also, the costate of this problem is given by $\lambda(t) = F(t)\nu$, where ν is a constant parameter.[6] Hence, we obtain

$$u_z(t) = \nu f_2(t) = \nu t_g(t) \tag{14}$$

As can be observed in Eqs. (10) and (14), the parameter $t_g(t)$ plays a key role in studying the OGL of missiles with varying velocity.

To gain an insight into the significance of $N(t)$, consider the case of a stationary target. Assuming small LOS angles, we have

$$\sigma = z/R \tag{15}$$

Furthermore, $\sigma_m - \sigma$ is assumed to be small, so that $\dot{R} = -V_m$, and, therefore, $R = V_m t_g$. Now, differentiation of Eq. (15) gives

$$\dot{\sigma} = \frac{-z\dot{R} + \dot{z}R}{R^2} = \frac{z + V_z t_g}{V_m t_g^2} = \frac{\mathrm{ZEM}}{V_m t_g^2}$$

Therefore, the OGL can be expressed in terms of $\dot{\sigma}$ as

$$u_z = \left(N/t_g^2\right)\mathrm{ZEM} = NV_m\dot{\sigma} \tag{16}$$

Here, we observe that the OGL for time-varying missile velocity is nothing but a PNG law with a time-varying guidance gain $N(t)$.

In the sequel, the relationship between $t_g(t)$ and the missile velocity profile is investigated in detail. Also, the effects of $t_g(t)$ on $N(t)$ are analyzed.

Characteristics of $t_g(t)$

Recall that $t_g(t)$ is defined by

$$t_g(t) = \frac{\int_t^{t_f} V_m(s)\,\mathrm{d}s}{V_m(t)} = \frac{\text{distance to go}}{\text{present missile velocity}}$$

Now define

$$\eta(t) = \frac{t_g(t)}{t_{\mathrm{go}}(t)}$$

We are to study the characteristics of t_g by investigating the trend of $\eta(t)$ in relation to the future missile velocity profile. We see that $\eta(t)$ is the ratio of the area under the curve of $V_m(s)$, $t \le s \le t_f$ to the area of the rectangle formed by $V_m(t)$ and $t_{\mathrm{go}}(t)$. In the following, we consider a class of velocity profiles that satisfies the assumptions 1) $V_m(t)$ is positive and continuous, and 2) $A_m(t) \equiv \mathrm{d}V_m(t)/\mathrm{d}t$ is finite and piecewise continuous. Then, property 1, described below, is an immediate consequence from the definition and assumptions.

Property 1:
i) $\eta(t) > 0$.
ii) $\lim_{t \to t_f} \eta(t) = 1$.
iii) $\eta(t) > 1$ for $t < t_f$ if $A_m(s) > 0$ for all $s \in [t, t_f]$.
iv) $\eta(t) < 1$ for $t < t_f$ if $A_m(s) < 0$ for all $s \in [t, t_f]$.
From the definition of $\eta(t)$, we obtain

$$\dot{\eta} = [(\eta - 1)/t_{go}] - (A_m/V_m)\eta \tag{17}$$

Backward integration of this equation together with $\dot{V}_m = A_m$ gives a numerical solution for $\eta(t)$. The boundary conditions are given by $\eta(t_f) = 1$ and $V_m(t_f) = V_f$. However, we are more interested in deriving some conditions that can be used to determine the trend of $\eta(t)$, specifically, the sign of $\dot{\eta}(t)$, without direct computation of $\eta(t)$. In this respect, we first note the following properties, which can be seen easily from Eq. (17).

Property 2:
i) If $\eta(t) > 1$ and $A_m(t) < 0$, then $\dot{\eta}(t) > 0$.
ii) If $\eta(t) < 1$ and $A_m(t) > 0$, then $\dot{\eta}(t) < 0$.

To derive more useful conditions, observe that for a given t, there exists a constant-acceleration velocity profile defined over $[t, t_f]$, denoted as $V_m^*(s; t)$, such that $V_m^*(t; t) = V_m(t)$ and

$$\int_t^{t_f} V_m^*(s; t)\,\mathrm{d}s = \int_t^{t_f} V_m(s)\,\mathrm{d}s \tag{18}$$

Let $\alpha^*(t)$ be the slope of $V_m^*(s; t)$. The value of $\alpha^*(t)$ can be computed easily from Eq. (18) as

$$\alpha^* = \frac{2(\eta - 1)V_m}{t_{go}} \tag{19}$$

Note that

$$\eta = 1 + \frac{\alpha^* t_{go}}{2V_m} \tag{20}$$

Property 3:
i) If $\eta(t) > 1$ and $A_m(t) \geq \alpha^*(t)$, then $\dot{\eta}(t) < 0$.
ii) If $\frac{1}{2} < \eta(t) < 1$ and $A_m(t) \leq \alpha^*(t)$, then $\dot{\eta}(t) > 0$.
iii) If $0 < \eta(t) < \frac{1}{2}$ and $A_m(t) \geq \alpha^*(t)$, then $\dot{\eta}(t) < 0$.

Proof:
i) Rewrite Eq. (17) as

$$\dot{\eta} = \frac{\eta - 1}{t_{go}} - \frac{\alpha^* \eta}{V_m} - \frac{\left(A_m - \alpha^*\right)\eta}{V_m}$$

Substitution of Eq. (20) into the preceding expression gives

$$\dot{\eta} = -\frac{\alpha^*}{2V_m}\left(1 + \frac{\alpha^* t_{go}}{V_m}\right) - \frac{\left(A_m - \alpha^*\right)\eta}{V_m}$$

Now, $\eta(t) > 1$ implies that $\alpha^*(t) > 0$ [see Eq. (19)]. Hence, if $A_m(t) > \alpha^*(t)$, then $\dot{\eta}(t) < 0$.

ii) If $\frac{1}{2} < \eta(t) < 1$, then $\alpha^*(t) < 0$ and $|\alpha^* t_{go}/V_m| < 1$ [see Eq. (20)]. Therefore, if $A_m(t) < \alpha^*(t)$, then $\dot{\eta}(t) > 0$.

iii) If $0 < \eta(t) < \frac{1}{2}$, then $\alpha^*(t) < 0$ but $\alpha^* t_{go}/V_m < -1$. [This case occurs when $V_m^*(t_f; t) < 0$.] Hence, if $A_m(t) > \alpha^*(t)$, then $\dot{\eta}(t) < 0$. □

To compute $\alpha^*(t)$, we need to know $\eta(t)$. However, by using the fact that the area under $V_m^*(s; t)$ is equal to that under $V_m(s)$, a graphic approximation of $V_m^*(s; t)$ can be obtained without computing $\eta(t)$.

Let $V_{max}(t)$ and $V_{min}(t)$ be defined by

$$V_{max}(t) = \max_{t \leq s \leq t_f} V_m(s), \qquad V_{min}(t) = \min_{t \leq s \leq t_f} V_m(s)$$

Property 4:
i) $\dot{\eta}(t) < 0$ if $A_m(t) > [V_{max}(t) - V_m(t)]/t_{go}(t)$.
ii) $\dot{\eta}(t) > 0$ if $A_m(t) < [V_{min}(t) - V_m(t)]/t_{go}(t)$.

Proof:
i) If $A_m(t)t_{go}(t) > V_{max}(t) - V_m(t)$, then $A_m(t) > 0$ and

$$V_m(t) + A_m(t)t_{go}(t) > V_{max}(t) \geq V_m(s), \qquad t \leq s \leq t_f$$

Hence,

$$\int_t^{t_f} [V_m(t) + A_m(t)t_{go}(t)]\,\mathrm{d}s > \int_t^{t_f} V_m(s)\,\mathrm{d}s$$

or

$$[V_m(t) + A_m(t)t_{go}(t)]t_{go}(t) > V_m(t)t_g(t) = V_m(t)t_{go}(t)\eta(t)$$

which reduces to

$$E \equiv [(\eta - 1)/t_{go}] - (A_m/V_m) < 0$$

Hence, if $\eta > 1$, then

$$\dot{\eta} = [(\eta - 1)/t_{go}] - (A_m \eta/V_m) = E - (A_m/V_m)(\eta - 1) < 0$$

Also, if $\eta < 1$, then we apply property 2(ii) to obtain $\dot{\eta} < 0$ because $A_m > 0$.

ii) The proof is similar to that of (i) and is omitted here. □

Let $\bar{V}_m(s; t)$ denote the tangent line of $V_m(s)$ at $s = t$. Then, the terminal value of the tangent line is calculated as $\bar{V}_m(t_f; t) = V_m(t) + A_m(t)t_{go}(t)$. Hence, we observe that the conditions of property 4 can be checked simply by comparing $\bar{V}_m(t_f; t)$ with $V_{max}(t)$, or with $V_{min}(t)$, whereas those of property 3 are based on the comparison of $V_m^*(t_f; t)$ and $\bar{V}_m(t_f; t)$. An advantage of the conditions of property 4 is that they do not require the value of $\eta(t)$. Furthermore, the graphic analysis to determine the sign of $\dot{\eta}(t)$ is easier with property 4 than with property 3. Applicability of properties 3 and 4 depends on the shape of the velocity profile from t to t_f.

In the following, we consider the characteristics of $t_g(t)$ for several special cases:

1) Constant velocity: $t_g(t) = t_{go}(t)$; thus $\eta(t) = 1$.

2) Deceleration attributable to aerodynamic drag: A fair approximation of aerodynamic deceleration for supersonic conditions is given by

$$\dot{V}_m = -(1/\tau)V_m$$

where the value of τ typically ranges from 8 to 10.[7] By property 1(iv), we have $t_g(t) < t_{go}(t)$ (or $\eta(t) < 1$). Also, property 4(ii) implies that $\eta(t)$ is monotonically increasing. The explicit expression of $t_g(t)$ is obtained as

$$t_g = \tau\left[1 - e^{-(t_{go}/\tau)}\right]$$

3) Constant acceleration: Suppose that $\dot{V}_m = c$, $c > 0$. By properties 1(iii) and 3(i), we see that $\eta(t)$ is monotonically decreasing to 1. The expression of $\eta(t)$ for this case is already derived in Eq. (20) as

$$t_g = t_{go} + \frac{c t_{go}^2}{2V_m}$$

4) Typical velocity profiles: A typical missile velocity profile consists of a boost phase followed by a coasting phase, as shown in Fig. 2. In this figure, we assume that the intercept occurs during the coasting phase. Here, t_0 denotes the initial time, t_1 the time at which

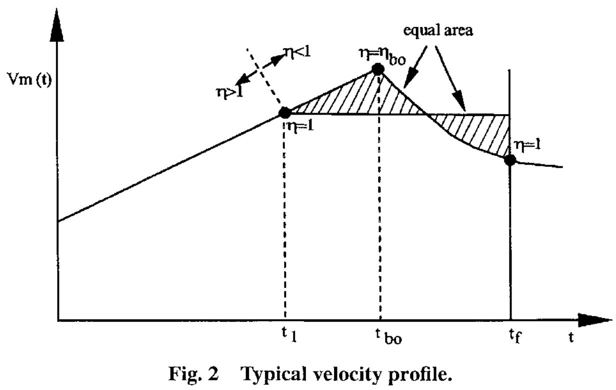

Fig. 2 Typical velocity profile.

$\eta(t) = 1$, t_{bo} the time at burnout, and t_f the time of intercept, respectively. The boost phase is approximated as a constant acceleration flight, whereas the coasting phase is modeled as case 2, discussed above. The characteristics of $\eta(t)$ during the coasting phase already have been discussed in case 2; $\eta(t)$ is monotonically increasing to 1 as t goes to t_f. Although the result of case 3 is not useful for the boost phase, property 4(i) implies that $\eta(t)$ is monotonically decreasing for $t < t_{bo}$. Hence, it is clear that $\eta(t)$ takes its minimum at burnout. This argument is generally true for single-booster missiles, and for booster-sustainer missiles if the time delay between booster burnout and sustainer ignition is sufficiently small. We can easily show that the value of $\eta_{bo} \equiv \eta(t_{bo})$ is bounded by

$$\frac{V_m(t_f)}{V_m(t_{bo})} < \eta_{bo} < \frac{1}{2}\left[1 + \frac{V_m(t_f)}{V_m(t_{bo})}\right] < 1$$

Characteristics of *N*(*t*)

Recall that the optimal guidance gain for time-varying missile velocity is given by

$$N(t) = \frac{t_g^3(t)}{\int_t^{t_f} t_g^2(s)\,ds} \tag{21}$$

In this section, the relationship between $\eta(t)$ and $N(t)$ is investigated for an arbitrary velocity profile. Now define

$$\eta_{min}(t) = \min_{t \le s \le t_f} \eta(s), \qquad \eta_{max}(t) = \max_{t \le s \le t_f} \eta(s)$$

Property 5:

i) $3\eta^3(t)/\eta_{max}^2(t) < N(t) < 3\eta^3(t)/\eta_{min}^2(t)$

ii) $\lim_{t\to t_f} N(t) = 3$

Proof:

i) Note that for $t \le s \le t_f$,

$$t_{go}^2(s)\eta_{min}^2(t) < t_g^2(s) = t_{go}^2(s)\eta^2(s) < t_{go}^2(s)\eta_{max}^2(t)$$

Hence,

$$\frac{t_{go}^3\eta^3(t)}{\eta_{max}^2(t)\int_t^{t_f} t_{go}^2(s)\,ds} < N(t) < \frac{t_{go}^3\eta^3(t)}{\eta_{min}^2(t)\int_t^{t_f} t_{go}^2(s)\,ds},$$

which reduces to

$$\frac{3\eta^3(t)}{\eta_{max}^2(t)} < N(t) < \frac{3\eta^3(t)}{\eta_{min}^2(t)}$$

ii) As t goes to t_f, $\eta(t)$ goes to 1 [see property 1(ii)]. Hence, $\eta_{max}(t)$ and $\eta_{min}(t)$ also approach 1. Therefore, by the inequality of (i), we have $\lim_{t\to t_f} N(t) = 3$. □

Property 6:

i) If $\eta(s)$ is monotonically decreasing in $[t, t_f]$, then $3\eta(t) < N(t) < 3\eta^3(t)$ for any $t \in [t, t_f)$.

ii) If $\eta(s)$ is monotonically increasing in $[t, t_f]$, then $3\eta^3(t) < N(t) < 3\eta(t)$ for any $t \in [t, t_f)$.

Proof:

i) If $\eta(t)$ is monotonically decreasing, then $\eta_{max}(t) = \eta(t)$ and $\eta_{min}(t) = 1$. Hence, by property 5(i), it is clear that $3\eta(t) < N(t) < 3\eta^3(t)$.

ii) The proof is similar to that of (i). □

In the following, we consider again the special cases treated previously:

1) Constant velocity: $t_g(t) \equiv t_{go}(t)$ and $N(t) \equiv 3$, which is the case of proportional navigation.

2) Deceleration attributable to aerodynamic drag: The guidance gain $N(t)$ is derived as

$$N = \frac{k^3}{\ln[1/(1-k)] - k - \frac{1}{2}k^2}$$

where $k = t_g/\tau = 1 - e^{-t_{go}/\tau}$. Note that $0 \le k \le 1$ and that k monotonically decreases to 0 as $t \to t_f$. Also, we can show that $dN/dk < 0$. Thus, $N(t)$ monotonically increases to 3 as $t \to t_f$.

3) Constant acceleration: For this case, $N(t)$ is obtained as

$$N = \frac{3(1-\rho^2)^3}{2(3 - 8\rho + 6\rho^2 - \rho^4)\rho^2}$$

where $\rho = V_m(t)/V_m(t_f)$. Using this expression, we can show that $dN/d\rho \le 0$. Because ρ monotonically increases to 1 as $t \to t_f$ (positive axial acceleration assumed), we conclude that $N(t)$ monotonically decreases to 3.

4) Typical velocity profiles: Consider again the velocity profile shown in Fig. 2. On the basis of the history of $\eta(t)$, we observe that

a) For $t_0 \le t \le t_1$ (front part of boosting phase), $\eta_{max}(t) = \eta(t)$ and $\eta_{min}(t) = \eta_{bo}$, so that $3\eta < N < 3\eta^3/\eta_{bo}^2$ [property 5(i)].

b) For $t_1 \le t \le t_{bo}$ (the rest of boosting phase), $\eta_{max}(t) = 1$ and $\eta_{min}(t) = \eta_{bo}$. Hence, $3\eta^3 < N < 3\eta^3/\eta_{bo}^2$.

c) For $t_{bo} \le t < t_f$ (coasting phase), $\eta_{max}(t) = 1$ and $\eta_{min}(t) = \eta(t)$, so that $3\eta^3 < N < 3\eta$.

Optimum Launch-Angle Computation

The optimum launch angle, denoted as σ_L, is the angle that gives a straight-line flight path to the intercept point, which is, for convenience, referred to as the collision path. The computation of the collision path of the missile provides an initial estimate of t_{go} as well as the launch angle. The following development for the optimum launch-angle computation is done in the same manner as in the paper by Baba et al.[5]

Let $t_{go,L}$ denote the time to go determined from the collision path. With the time of launch set to $t = 0$, the geometry of the collision path gives

$$\left[\int_0^{t_{go,L}} V_m(s)\,ds\right]\sin\sigma_L = t_{go,L}V_t(0)\sin\sigma_t(0) + \int_0^{t_{go,L}}\int_0^s a_{tz}(v)\,dv\,ds + Z(0) \tag{22}$$

$$\left[\int_0^{t_{go,L}} V_m(s)\,ds\right]\cos\sigma_L = t_{go,L}V_t(0)\cos\sigma_t(0) + \int_0^{t_{go,L}}\int_0^s a_{tx}(v)\,dv\,ds + X(0) \tag{23}$$

where $a_{tx} = (d/dt)(V_t\cos\sigma_t)$. These two equations can be numerically solved to give $t_{go,L}$ and σ_L. For example, for the constant-velocity target, we obtain from Eqs. (22) and (23)

$$\left[\int_0^{t_{go,L}} V_m(s)\,ds\right]^2 = t_{go,L}^2V_t^2 + 2t_{go,L}V_tR(0)\cos[\sigma_t - \sigma(0)] + R^2(0) \tag{24}$$

where we use the fact that the angle between the target velocity vector and the target-to-missile range vector is $\pi - [\sigma_t - \sigma(0)]$. Because σ_L does not appear in Eq. (24), we first solve this equation for $t_{go,L}$ and use Eq. (22) or (23) to obtain σ_L. A numerical zero-finding algorithm such as the secant method or Newton's method can be used for solving Eq. (24). For an accelerating target, a similar method is used to solve Eqs. (22) and (23). For practical reasons (it is impossible to predict the future target acceleration profile), however, a_{tz} and a_{tx} are taken to be constant for this case. The collision path thus obtained is not exact, but has been shown in computer simulations to be good enough for guidance-law implementation.

Computation of t_{go}

Because of launch error, the missile does not precisely fly along the path determined by the initial collision path. Therefore, an on-line computation of t_{go} is required to implement the OGL derived in this paper. Once t_{go} is determined, another required variable, t_g, can be evaluated by using the given missile velocity profile. Recall that the method frequently used for the computation of t_{go} is

$$t_{go} \approx \frac{R}{V_{c,LOS}} = \frac{X}{V_{cx}} \tag{25}$$

where $V_{c,\mathrm{LOS}}$ is the closing velocity along the LOS and V_{cx} is the x-axis component of $V_{c,\mathrm{LOS}}$. However, this method is not adequate for the case of time-varying missile velocity because Eq. (25) is valid only under the assumption that V_c is constant.

In the following, we suggest a more accurate method for on-line computation of t_{go}. The method is based on the assumption that the missile nullifies its heading error instantly to return to the collision path. The computation of t_{go} is then equivalent to that of the collision path at every instant. With the OGL, the missile always tries to reduce the heading error. Hence, this is a sound assumption, especially with a small initial heading error. Therefore, the numerical method used for launch-angle computation also can be used for determining t_{go}; for example, for a constant-velocity target,

$$\left[\int_t^{t+t_{go}} V_m(s)\,\mathrm{d}s\right]^2 = t_{go}^2 V_t^2 + 2t_{go} V_t R(t)\cos[\sigma_t - \sigma(t)] + R^2(t) \tag{26}$$

Note that this method is the same, in principle, as the one of Baba et al.[5] and that it consistently gives an underestimate of t_{go} when the target acceleration is perfectly known and constant, because the collision path is the shortest path from the current missile position to the intercept point. Numerical results, as shown in the simulation study, demonstrate excellent performance of the proposed method.

Implementation Aspects

To implement the OGL of Eq. (10), the missile requires the following: 1) an active radar seeker, 2) a target-tracking filter based on radar measurements, 3) determination of flight-path angle (or attitude and angle of attack), and 4) predicted missile velocity profile.

In addition to the foregoing, information on the actual missile longitudinal acceleration will be useful when on-line modification of the given missile velocity profile is desired. A formal procedure for guidance command generation is as follows:

1) Compute t_{go}.
2) Compute $t_g(t)$, $G(t)$, and ZEM.
3) Compute u_z and $u = u_z/\cos\sigma_L$.

Note that the last double integral in ZEM [Eq. (13)] cannot be performed in practice unless the future target acceleration history is known beforehand. Therefore, as done in the optimum launch angle and t_{go} computations, the best we can do is to assume that the target acceleration at the present time is maintained throughout the engagement and to replace the double integral by $\frac{1}{2}a_{tz}t_{go}^2$. Then, the guidance law in this case becomes

$$u_z = \left(N/t_g^2\right)\left[z + t_{go}V_z + (t_{go} - t_g)V_m\sin\sigma_m + \tfrac{1}{2}t_{go}^2 a_{tz}\right] \tag{27}$$

When we restrict ourselves to the case of constant-velocity target, we may use the approximate relations for real-time implementation of the guidance law expressed as

$$z = R\sigma, \qquad V_z = \dot{z} = \dot{R}\sigma + R\dot{\sigma}$$

In this case, the guidance command can be expressed in terms of seeker measurements:

$$u_z = \left(N/t_g^2\right)[(R + \dot{R}t_{go})\sigma + Rt_{go}\dot{\sigma} + (t_g - t_{go})V_m\sin\sigma_m] \tag{28}$$

In practice, t_{go} is updated every guidance cycle, and t_f may vary as t_{go} goes to 0. Other error sources also may produce variations in the estimated value of t_f; therefore, a real-time computation of $t_g(s)$ for all $s \in [t, t_f]$ and

$$G(t) = -\int_t^{t_f} t_g^2(d)\,\mathrm{d}s$$

is required.

Suppose that the guidance computer has a priori information of $V_m(t)$ and

$$D_m(t) = \int_0^t V_m(s)\,\mathrm{d}s$$

in table form. For a given t,

$$t_g(t) = \frac{D_m(t_f) - D_m(t)}{V_m(t)} \tag{29}$$

and

$$G(t) = \int_t^{t_f}\left[\frac{D_m^2(t_f) - 2D_m(t_f)D_m(s) + D_m^2(s)}{V_m^2(s)}\right]\mathrm{d}s$$

or

$$G(t) = D_m^2(t_f)[I_0(t_f) - I_0(t)] - 2D_m(t_f)[I_1(t_f) - I_1(t)] + [I_2(t_f) - I_2(t)] \tag{30}$$

where $I_0(t)$, $I_1(t)$, and $I_2(t)$ are defined as

$$I_0(t) = \int_0^t \frac{1}{V_m^2(s)}\,\mathrm{d}s, \qquad I_1(t) = \int_0^t \frac{D_m(s)}{V_m^2(s)}\,\mathrm{d}s$$

$$I_2(t) = \int_0^t \frac{D_m^2(s)}{V_m^2(s)}\,\mathrm{d}s$$

Hence, if the guidance computer has additional tables for $I_0(t)$, $I_1(t)$, and $I_2(t)$ in addition to $V_m(t)$ and $D_m(t)$, then the real-time computation of guidance command is possible without integration even for the case of varying t_f.

Simulation Results

In this simulation study, we assume no guidance system lag and perfect knowledge of the missile velocity profile throughout the engagement. We consider a surface-to-air missile engagement scenario as follows: The missile has an initial velocity of 340 m/s, accelerates for the first 2 s at the rate of 340 m/s^2, and then decelerates

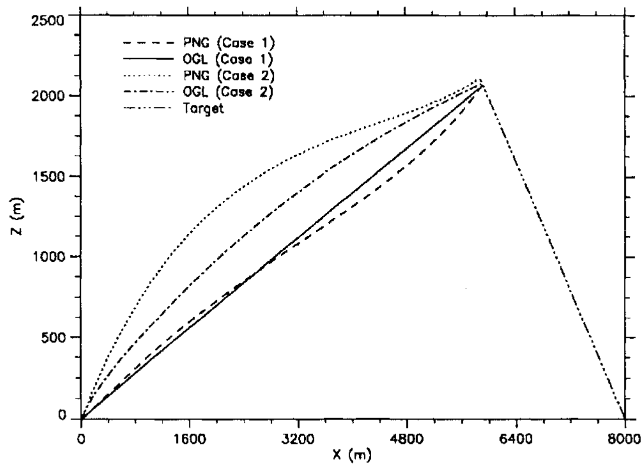

a) Missile and target trajectories

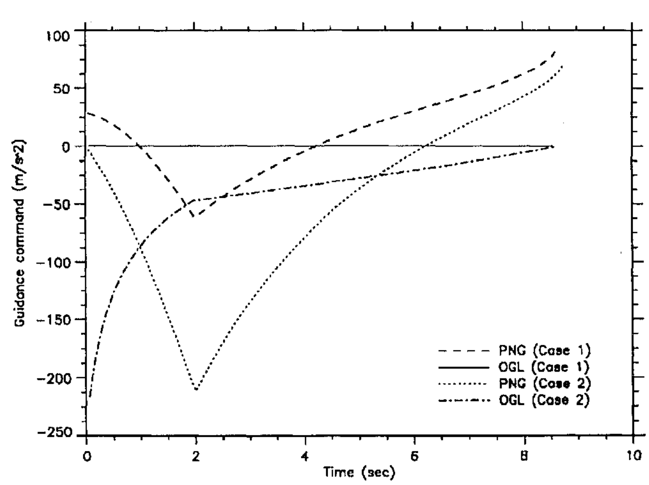

b) Missile acceleration histories

Fig. 3 Scenario 1: constant-velocity target.

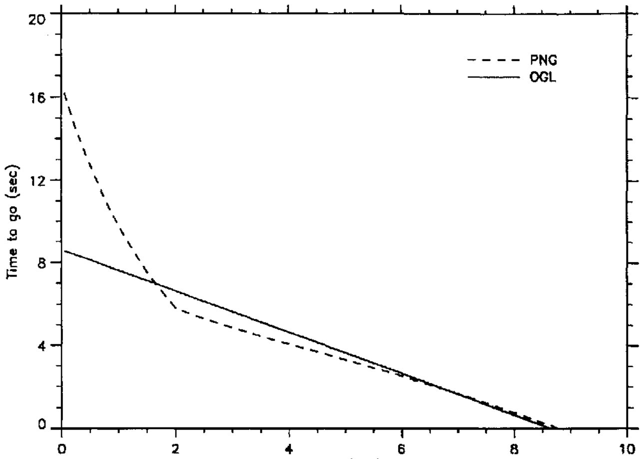

Fig. 4 Time-to-go (t_{go}) computation results for case 2 in scenario 1.

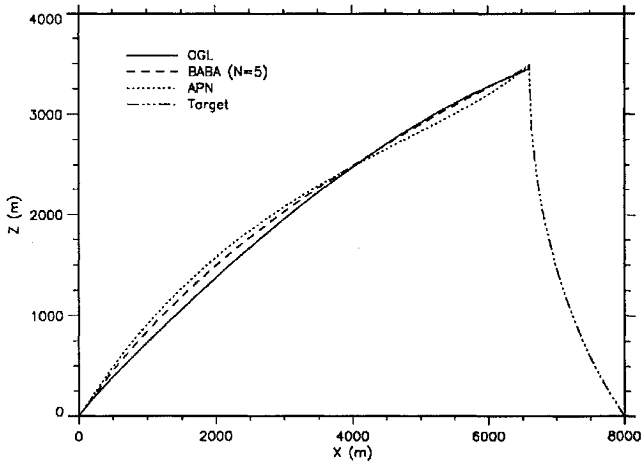

a) Missile and target trajectories

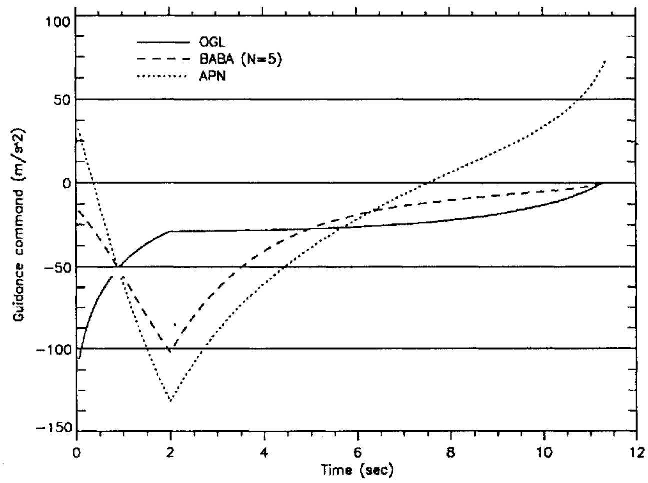

b) Missile acceleration histories

Fig. 5 Scenario 2 with the launch angle 15 deg off the optimum value (maneuvering target).

according to $\dot{V}_m = -(1/10)V_m$. In scenario 1, the target flies in the direction 135 deg away from the initial LOS with a constant velocity of 340 m/s. In scenario 2, the target exerts a circular motion with an acceleration. The initial range is 8 km and the initial LOS is taken as the reference line.

Figure 3 illustrates the performance of two guidance laws for scenario 1: a PNG law in the form of $u = (3/t_{go}^2)(z+t_{go}v_z)$ and the OGL of Eq. (28) with $a_{tz} = 0$. The computation of t_{go} is performed by using Eq. (25) for PNG and by the method suggested in this paper for OGL, respectively. Two cases of the initial flight-path angle $\sigma_m(0)$ are considered: case 1 uses the result of the optimum launch-angle computation discussed in this paper, and case 2 takes the usual value of $V_t \sin\sigma_t / V_m(0)$. Figure 3 shows superior performance of OGL over PNG for both cases. Figure 4 shows an excellent performance of the t_{go} computation method used for OGL.

In Fig. 5, OGL is also compared to APN, $u = (3/t_{go}^2)(z + t_{go}v_z + \frac{1}{2}t_{go}^2 a_{tz})$, and to the guidance law of Baba et al. (more specifically, APXGL with $N = 5$ in Ref. 5 for scenario 2). For a fair comparison, we have used the same t_{go} computation method of this paper for all guidance laws. In this figure, we observe that guidance commands of OGL and Baba's decrease to 0 as the missile approaches the target, which is one of the most desirable properties of a guidance system. On the other hand, the guidance command of APN becomes larger in the end. In fact, the acceleration command generated by OGL reduces to zero in all simulation runs as t goes to t_f, which is, in fact, expected from Eq. (14). We note that the guidance law of Baba et al.[5] often fails to yield this property when the guidance gain is not large enough, for example, $N = 3$. The initial acceleration command of OGL is found to be large in the simulation runs. This is because OGL tries to minimize the overall control efforts, applying larger acceleration commands when the missile velocity is lower. The control efforts

$$\int_0^{t_f} [u(t)]^2 \, dt$$

computed for scenario 2 are 11,918 for OGL, 36,699 for APN, and 19,370 for Baba's guidance law. Miss distances in all simulations are nil because zero guidance system lag and unlimited missile acceleration capability are assumed.

Concluding Remarks

In this paper, we have investigated an OGL for missiles with time-varying velocity. The closed-form solution has been derived, and properties of the key variables, including the time-varying time-to-go and gain functions of the solution, have been studied. We have also explored some issues in implementing the OGL, in particular, the computational problem for the optimum launch angle (or the collision path) and the integral of $[t_g(t)]^2$. The overall guidance algorithm developed is shown in computer simulations to outperform the OGLs for constant missile velocity, i.e., proportional navigation and augmented proportional navigation. The proposed guidance law also shows a desirable property that the acceleration command—under the assumption of no guidance system lag and perfect knowledge of the necessary information—reduces to zero as t approaches t_f. Further studies are still to be done in areas such as analysis of performance degradation attributable to missile velocity variations and, if the longitudinal missile acceleration is available, on-line compensation for the deviation of the actual missile velocity profile from the stored (predicted) one. The tendency of large initial guidance commands of the proposed guidance law is not desirable. Because it might not be possible to realize large acceleration commands in the early stage of the engagement, some research efforts are being put to remedy the problem.

References

[1]Green, A., Shinar, J., and Guelman, M., "Game Optimal Guidance Law Synthesis for Short Range Missiles," *Journal of Guidance, Control, and Dynamics*, Vol. 15, No. 1, 1992, pp. 191–197.

[2]Nazaroff, G. J., "An Optimal Terminal Guidance Law," *IEEE Transactions on Automatic Control*, Vol. AC-21, No. 3, 1976, pp. 407, 408.

[3]Riggs, T. L., Jr., "Linear Optimal Guidance for Short Range Air-to-Air Missiles," *Proceedings of IEEE National Aerospace and Electronics Conference* (Oakland, MI), Vol. 2, Inst. of Electrical and Electronics Engineers, New York, 1979, pp. 757–764.

[4]Hull, D. G., Radke, J. J., and Mack, R. E. "Time-to-Go Prediction for Homing Missiles Based on Minimum-Time Intercepts," *Journal of Guidance, Control, and Dynamics*, Vol. 14, No. 5, 1991, pp. 865–871.

[5]Baba, Y., Takehira T., and Takano, H., "New Guidance Law for a Missile with Varying Velocity," *Proceedings of the AIAA Guidance, Navigation, and Control Conference*, AIAA, Washington, DC, 1994, pp. 207–215 (AIAA Paper 94-3565).

[6]Bryson, A. E., and Ho, Y. C., *Applied Optimal Control*, Wiley, New York, 1975, Chap. 5.

[7]Garnell, P., and East, D. J., *Guided Weapon Control Systems*, 2nd ed., Pergamon, Oxford, England, UK, 1980.